Nanoscale Res Lett (2010) 5:769–772
DOI 10.1007/s11671-010-9555-8

NANO EXPRESS

Vacancy-Mediated Magnetism in Pure Copper Oxide Nanoparticles

Daqiang Gao · Jing Zhang · Jingyi Zhu · Jing Qi · Zhaohui Zhang · Wenbo Sui · Huigang Shi · Desheng Xue

Received: 8 December 2009 / Accepted: 28 January 2010 / Published online: 16 February 2010

Abstract Room temperature ferromagnetism (RTF) is observed in pure copper oxide (CuO) nanoparticles which were prepared by precipitation method with the post-annealing in air without any ferromagnetic dopant. X-ray photoelectron spectroscopy (XPS) result indicates that the mixture valence states of Cu^{1+} and Cu^{2+} ions exist at the surface of the particles. Vacuum annealing enhances the ferromagnetism (FM) of CuO nanoparticles, while oxygen atmosphere annealing reduces it. The origin of FM is suggested to the oxygen vacancies at the surface/or interface of the particles. Such a ferromagnet without the presence of any transition metal could be a very good option for a class of spintronics.

Keywords CuO · Nanoparticles · X-ray photoelectron spectroscopy · Room temperature ferromagnetism

Introduction

Recently, integration of semiconductor with ferromagnetic function has been focused on in spintronics because of the difficulties associated with the injection of spins from magnetic metal into nonmagnetic semiconductors in conventional spintronic devices. Many groups have found RTF in transition or rare earth metal–doped compound semiconductors such as TiO_2 [1], ZnO [2], SnO_2 [3], and In_2O_3 [4]. When groups of people try to explain the FM in transition metal–doped semiconducting oxides, an unexpected FM was reported in pure HfO_2 thin film [5], which challenges the understanding of magnetism for the researchers. Hong et al. suggested that oxygen vacancies were key factors in introducing FM to HfO_2 [6], while Pemmaraju and Sanvito [7] suggested that the origin of RTF in HfO_2 was due to defects on Hf sites. Hu et al. [8] presented that RTF observed in pure MgO results from cation vacancies. Elfimov et al. [9] suggested that a small concentration of Ca vacancies in CaO can also induce FM based on results of the ab initio electronic structure calculation, which could be a path to new ferromagnets. Recently, similar FM has been reported in other pure semiconductor materials, such as TiO_2, ZnO, SnO_2, In_2O_3, Al_2O_3, and CeO_2, where the origin of FM is believed to be oxygen defects [10, 11].

CuO, as a narrow band gap p-type semiconductor, has been recognized as an industrially important material for a variety of practical applications, such as catalysis, batteries, solar energy conversion, gas sensing, and field emission [12–14]. Therefore, the synthesis and study of CuO nanostructures should be of practical and fundamental importance. Apart from this, if one can find FM without any magnetic impurity doping, this may bring a new opportunity to the field of spintronics because there will be no issues due to clustering or precipitation of dopants. Indeed, Punnoose et al. and Mishra et al. [15, 16] represented the presence of an exchange interaction between the ferromagnetic surface and the antiferromagnetic core. Recently, Xiao et al. and Shang et al. [17, 18] reported the observation of RTF in CuO nanostructures. However, the FM in CuO remains controversial because most groups suggested that Cu atoms have no clustering tendency and Cu-based oxides are not ferromagnetic [19, 20]. Here, we synthesize CuO nanoparticles by a simple co-precipitation

D. Gao · J. Zhang · J. Zhu · J. Qi · Z. Zhang · W. Sui · H. Shi · D. Xue (✉)
Key Laboratory for Magnetism and Magnetic Materials of MOE, Lanzhou University, 730000 Lanzhou, People's Republic of China
e-mail: xueds@lzu.edu.cn

method to avoid the influences of substrate and the interface between film and substrate [21]. We found the CuO nanoparticles show RTF, and the origin of the FM is discussed.

Experiments

CuO nanoparticles were prepared by the precipitation technique with the post-oxidation annealing in air. Briefly, 3 g highly pure Cu $(NO3)_26H_2O$ was dissolved in 50 ml de-ionized water, and the NH_4OH solution was added into it gradually until the pH level reached 10. The mixture was stirred for 4 h at room temperature and then dried at 50°C for 6 h. In the end, the precursor was annealed at 800°C for 1 h in air. The morphologies of the nanoparticles were obtained by transmission electron microscopy (TEM, JEM-2010). X-ray diffraction (XRD, X' Pert PRO PHILIPS with Cu Kα radiation) was employed to study the structure of the particles. The doping levels and the bonding characteristics were determined by X-ray Photoelectron Spectroscopy (XPS, VG ESCALAB 210). The compositions of the particles were analyzed by inductively coupled plasma atomic emission spectrometer (IRIS, ER/S). The measurements of magnetic properties were made using Quantum Design MPMS magnetometer based on superconducting quantum interference device (SQUID) and the vibrating sample magnetometer (VSM, Lakeshore 7304).

Results and Discussions

Figure 1a shows the typical XRD pattern of the CuO nanoparticles. All diffraction peaks can be indexed as the typical monoclinic structure, and no extra diffraction peaks of other phases are observed. Refinement gives lattice constants are $a = 4.6881(8)$ Å, $b = 3.4293(1)$ Å, $c = 5.1354(1)$ Å, and $\beta = 99.304(9)°$. Using the Scherrer formula and the full width at half maximum of the main peak, the average crystalline size is estimated to be around 26 nm. Figure 1b gives the morphology images of the sample captured by TEM, and it can be seen that the particles congregate together and the size of which is about 150 nm. Figure 1c shows the high-resolution TEM image of the corresponding CuO nanoparticles. The lattice fringes between the two adjacent planes are 0.253 nm apart, which is equal to the lattice constant of the standard CuO in (002) plane.

The magnetization versus magnetic field (*M-H*) curves for the CuO nanoparticles recorded at 10 and 300 K are shown in Fig. 2, which were investigated using the SQUID magnetometer, and the paramagnetic (PM) signal of the sample and the holder were deducted. The hysterics loop of

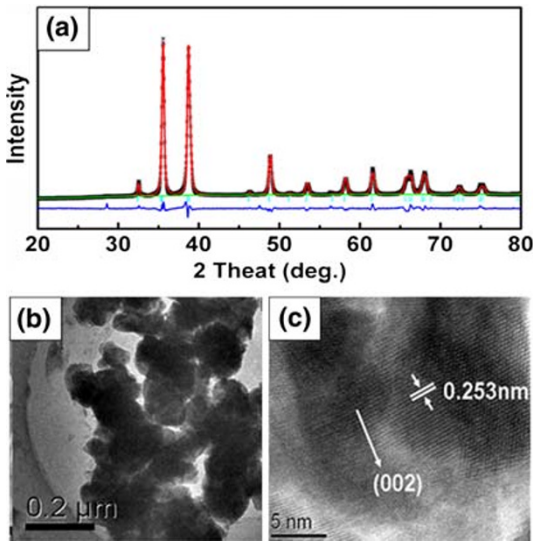

Fig. 1 **a** Refined XRD pattern **b** TEM and **c** high-resolution TEM images of the CuO nanoparticles annealed at 800°C for 1 h

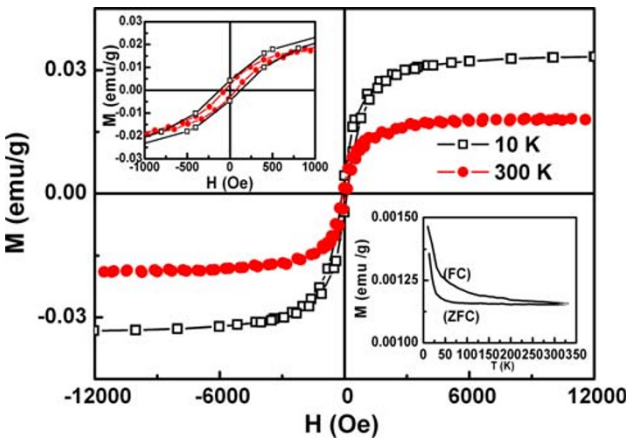

Fig. 2 *M-H* curves of CuO nanoparticles annealed at 800°C recorded at 10 and 300 K, in which the paramagnetic signal of the sample and the holder have been deducted. The *top left inset* shows the magnification of the central part for *M-H* curves and the *bottom right inset* shows the FC-ZFC curve of CuO nanoparticles annealed at 800°C

300 K indicates that the sample has clearly RTF. The top left inset is the magnification of the central part for the *M-H* curves. It can be seen that the measured coercivities and the saturated magnetizations (M_s) of the CuO nanoparticles are 120 Oe, 0.018 emu/g, and 57 Oe, 0.032 emu/g at 10 and 300 K, respectively. The coercivities are smaller than that of report in reference 18 (331.39 and 175.88 Oe at 10 and 300 K, respectively). The zero-field-cooled (ZFC) and field-cooled (FC) magnetization curves in the temperature range of 2–330 K at the field of 100 Oe on CuO were shown in below inset of Fig. 2. The results indicate there is no blocking temperature in this temperature range, supporting that there is no contamination of ferromagnetic cluster. At the

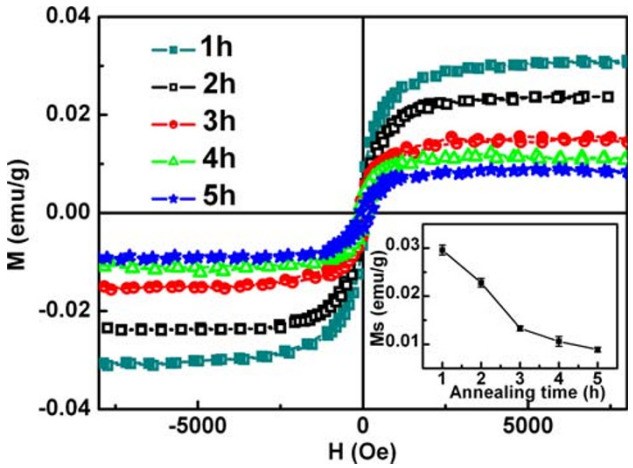

Fig. 3 *M-H* curves for CuO nanoparticles annealed at 800°C for different times. The *inset* shows the variation of M_s

same time, we can conclude that the Curie temperature of the sample is above 300 K. Figure 3 shows the *M-H* curves of the CuO nanoparticles annealing at 800°C for different annealing time, and the variation of M_s is shown in the inset. The PM signal of the sample and the holder also have been deducted. It can be seen that as the annealing time increasing, the magnetization decreases gradually. And the reason will be discussed later. In addition, it is noticed that magnetic measurements were reproducible for all the CuO samples synthesized repeatedly in different batches under identical experimental conditions.

Several publications show contamination is a possible source of the FM in HfO_2, TiO_2, SnO_2, etc. [22, 23]. In explaining the origin of FM in the CuO nanoparticles, a careful consideration whether the contamination is responsible for the FM has to be undertaken. All the processes of experiments were carried out very carefully. And the capsules used to hold the samples during the magnetic measurements were also checked carefully and showed no ferromagnetic signals. The result of inductively coupled plasma (ICP) indicates that elements such as Fe (Co) exists in our sample are about 2×10^{-6} at.%, which may come from the precursor material of $Cu(NO3)_2{\cdot}6H_2O$. However, magnetic measurement indicates that the precursor particles are PM, and it did not influence the magnetic properties of the CuO nanoparticles in agreement with other reports [24]. Therefore, we suggest that the observed FM is intrinsic in all samples. So we must reconsider the possibility origin of FM which was previously assumed for the other ferromagnetic undoped oxides: FM due to oxygen vacancies and/or defects [5–11].

Figure 4 presents the survey scan and Cu 2*p* core level binding energy spectra of the CuO nanoparticles. All the indexed peaks are corresponding to C, O, and Cu as shown in Fig. 4 survey spectrum. The inset of Fig. 4 shows Cu 2p XPS spectra of CuO nanoparticles. The strong fitting peaks at around 932.1 and 952.3 eV for Cu^{1+} 2p3/2 and 2p1/2 peaks and 933.4 eV and 954.4 eV for Cu^{2+} 2p3/2 and 2p1/2 peaks are much closer to the other report [20], which reveals that the chemical valences of Cu at the surface of the CuO nanoparticles are mixture valence states of +1 and +2. There are no extrinsic magnetic impurities in the undoped CuO, so the occurrence of FM is predominately due to a complex interplay of two different valence states of the copper ions at the surface of the particles with the oxygen vacancies and the associated defects.

In order to experimentally verify this prediction, vacuum and oxygen annealing were done for the CuO nanoparticles as other groups' method [25, 26]. Figure 5 shows the variation of M_s for CuO particles in different annealing conditions. At first, as-prepared CuO nanoparticles were annealed in vacuum atmosphere (0.001 Pa) at 400°C for 30 min, which is denoted as "vacuum" in the figure. It is seen that the FM of CuO particles enhances and the *Ms* reaches 0.024 emu/g. Then the sample was annealed in the rich oxygen atmosphere (the mix atmosphere of argon and oxygen) at 400°C for 30 min, which is denoted as "oxygen". And the M_s decreases to 0.007 emu/g. Finally, the FM increases again and the value of M_s reaches up to 0.021 emu/g after the sequential repeating annealing in vacuum. The *M-H* curves for the CuO nanoparticles of each annealing condition are shown in inset of Fig. 5, which were measured by VSM, and the PM signal of the sample and the holder have been deducted. Usually, the vacuum annealing effectively introduces oxygen vacancies into oxides, while the rich oxygen annealing reduce oxygen vacancies. It is found in our experiment that the FM of the CuO nanoparticles increases after annealing in vacuum condition and decreases after annealing in the rich oxygen

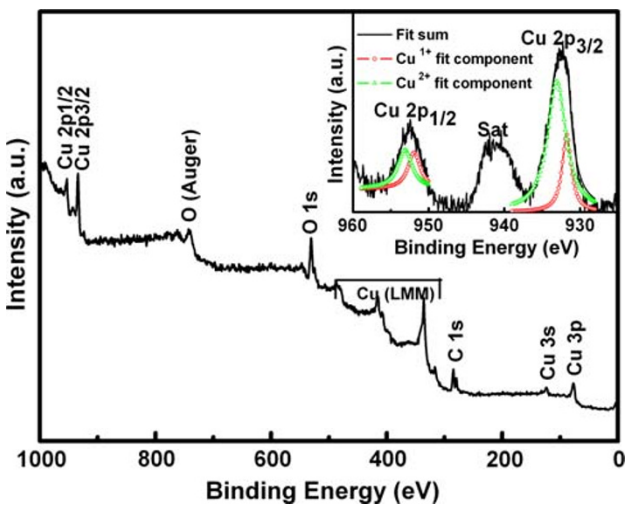

Fig. 4 The XPS spectra of CuO nanoparticles annealed at 800°C. The *inset* shows the Cu 2*p* core level binding energy spectra

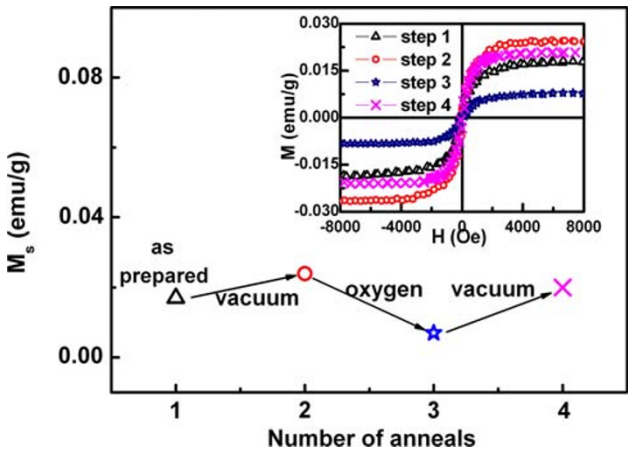

Fig. 5 The variation of M_s for CuO nanoparticles sequential annealed at different conditions in vacuum and oxygen atmosphere. The *inset* shows their *M-H* curves

atmosphere, which is corresponding to our previous report in ZnO nanoparticles [27].These results prove that the RTF of the undoped CuO nanoparticles originates from oxygen vacancies in our case. Theoretically speaking, the oxygen atoms can escape from the bondage of the chemical bond because of heating. Then the unpaired electrons show the abnormal spin phenomenon which could cause the magnetism. In addition, as the annealing time increases, the size of particle increases gradually and the particles aggregate together with the decreasing of the M_s, which indicate that oxygen vacancies at the surface/or interface of the particles are likely to be responsible for the FM in the CuO nanoparticles.

Summary

In summary, CuO nanoparticles were prepared by co-precipitation method with the post-annealing in air. The clear hysteresis loop is observed at room temperature in CuO nanoparticles, and the extrinsic impurity origin is excluded. The results of repeating annealing CuO nanoparticles in different conditions indicate that oxygen vacancies at the surface of the particles are likely to be responsible for the FM. Further theoretic investigations into the defects introducing FM are expected and our work is on the way.

Acknowledgments This work is supported by NSFC (Grant No.50671046 and No.50801033), National Science Fund for Distinguished Young Scholars (Grant No. 50925103) and the Fundamental Research Funds for the Central Universities (Grant No. Lzujbky-2009-162).

References

1. Y.B. Lin, Y.M. Yang, B. Zhuang, S.L. Huang, L.P. Wu, Z.G. Huang, F.M. Zhang, Y.W. Du, J. Phys. D Appl. Phys. **41**, 195007 (2008)
2. J. Qi, Y.H. Yang, L. Zhang, J.H. Chi, D.Q. Gao, D.S. Xue, Scripta Mater. **60**, 289 (2009)
3. L. Zhang, S.H. Ge, Y.L. Zuo, X.Y. Zhou, Y.H. Xiao, S.M. Yan, X.F. Han, Z.C. Wen, J. Appl. Phys. **104**, 123909 (2008)
4. N.H. Hong, J. Sakai, N.T. Huong, A. Ruyter, V. Brizé, J. Phys. Condens. Matter **18**, 6897 (2006)
5. M. Venkatesan, C.B. Fitzgerald, J.M.D. Coey, Nature (London) **430**, 630 (2004)
6. J.M.D. Coey, M. Venkatesan, P. Stamenov, C.B. Fitzgerald, L.S. Dorneles, Phys. Rev. B **72**, 024450 (2005)
7. C.D. Pemmaraju, S. Sanvito, Phys. Rev. Lett. **94**, 217205 (2005)
8. J.F. Hu, Z.L. Zhang, M. Zhao, H.W. Qin, M.H. Jiang, Appl. Phys.Lett. **93**, 192503 (2008)
9. I.S. Elfimov, S. Yunoki, G.A. Sawatzky, Phys. Rev. Lett. **89**, 216403 (2002)
10. A. Sundaresan, R. Bhargavi, N. Rangarajan, U. Siddesh, C.N.R. Rao, Phys. Rev. B **74**, 161306 (2006)
11. N.H. Hong, J. Sakai, N. Poirot, V. Brizé, Phys. Rev. B **73**, 132404 (2006)
12. K. Sanfra, C.K. Sarkar, M.K. Mukherjee, Thin Solid Films **213**, 226 (1992)
13. C.L. Carnes, K.J. Klabunde, J. Mol. Catal. A Chem. **194**, 227 (2003)
14. P. Dai, H.A. Mook, G. Aeppli, S.M. Hayden, F. Dogan, Nature **406**, 965 (2000)
15. A. Punnoose, M.S. Seehra, J. Appl. Phys. **91**, 10 (2002)
16. A. Punnoose, H. Magnone, J. Bonevich, M.S. Seehra, Phys. Rev. B. **64**, 174420 (2001)
17. D.J. Shang, K. Yu, Y.S. Zhang, J.W. Xu, J. Wua, Y.E. Xu, L.J. Li, Z.Q. Zhu, Appl. Surf. Sci. **255**, 4093 (2009)
18. H.M. Xiao, L.P. Zhu, X.M. Liu, S.Y. Fu, Solid State Commun. **141**, 431 (2007)
19. T. Ashutosh, S. Michael, K. Dhananjay, T.A. Jeremiah, Appl. Phys. Lett. **92**, 062509 (2008)
20. G.Z. Xing, J.B. Yi, J.G. Tao, T. Liu, L.M. Wong, Z. Zhang, G.P. Li, S.J. Wang, J. Ding, T.C. Sum, C.H.A. Huan, T. Wu, Adv. Mater. **20**, 3521 (2008)
21. P.J. Grace, M. Venkatesan, J. Alaria, J.M.D. Coey, G. Kopnov, R. Naaman, Adv. Mater. **21**, 71 (2009)
22. D.W. Abraham, M.M. Frank, S. Guha, Appl. Phys. Lett. **87**, 252502 (2005)
23. J.B. Yi, H. Pan, J.Y. Lin, J. Ding, Y.P. Feng, S. Thongmee, T. Liu, H. Gong, L. Wang, Adv. Mater. **20**, 1170 (2008)
24. M. Khalid, M. Ziese, A. Setzer, P. Esquinazi, M. Lorenz, H. Hochmuth, M. Grundmann, D. Spemann, T. Butz, G. Brauer, W. Anwand, G. Fischer, W.A. Adeagbo, W. Hergert, A. Ernst, Phys. Rev. B. **80**, 035331 (2009)
25. N. Khare, M.J. Kappers, M. Wei, M.G. Blamire, J.L. Macmanus-Driscoll, Adv. Mater. **18**, 1449 (2006)
26. K.R. Kittilstved, D.A. Schwartz, A.C. Tuan, S.M. Heald, S.A. Chambers, D.R. Gamelin, Phys. Rev. Lett. **97**, 037203 (2006)
27. D.Q. Gao, Z.H. Zhang, J.L. Fu, X. Yan, D.S. Xue, J. Appl. Phys. **105**, 113928 (2009)